FUNDAMENTAL ELECTROMAGNETIC PROPERTIES OF THE NEUTRON

Yu. A. Aleksandrov

This review is devoted mainly to experimental investigations of the fundamental electromagnetic properties of the neutron: electric charge, electric dipole moment, electromagnetic form factors, polarizability, and n-e interaction.

INTRODUCTION

The neutron was discovered in 1932 and probably had more effect on the development of physics than any other elementary particle. The discovery of the neutron initiated the age of nuclear physics, the rapid development of which in the middle of the 20th century led to the birth of nuclear technology and elementary particle physics.

We know a considerable amount about the neutron. Its interaction with nuclei has been fairly well investigated – without this knowledge there would be no nuclear reactors. We know its mass, spin, magnetic moment, and electric charge – the knowledge of these characteristics enables us to use the neutron as a very convenient tool for many investigations, such as the study of the structure of condensed media. In recent years, thanks to the efforts of many physicists, we have managed to build up at least a qualitative picture of the structure of the neutron. We have found that the neutron is a particle with a fairly complicated structure. At any rate, its behavior when it interacts with matter reveals properties which are characteristic of an extended particle. The neutron does not act directly on our sense organs and, hence, all that we know about it has been learned through its interaction with other particles and fields. There are four types of interaction: gravitational, weak, electromagnetic, and strong. The weakest of these is gravitational interaction. The neutron is the only particle with a rest mass which has been experimentally determined from its fall in the earth's gravitational field. There have been no surprises so far – the neutron behaves in the gravitational field like an ordinary macroscopic body.

Weak interaction is responsible for the decay of the neutron into a proton, electron, and antineutrino. Although neutron decay has been studied for a fairly long time, this field is still exceedingly attractive to experimenters. Even such a characteristic as the neutron half-life requires more accurate determination – the difference between different measurements is more than three times the measurement error.

Strong interactions are responsible for the reactions of neutrons with nuclei, and nuclei owe their very existence to strong interactions. Here there is a wealth of experimental material and probably even greater problems, which are unlikely to be settled without an understanding of strong interactions between elementary particles.

Finally, electromagnetic interaction, with the aid of which we have learned about such fundamental properties of the neutron as its electric charge, electric dipole moment, and electromagnetic structure, belongs to a region which we think we understand. So far, at least, we have discovered no effect which contradicts quantum electrodynamics. It is possible that the discovery of such an effect would be the starting point of a new theory, the development of which would lead to an understanding of strong interactions.

Joint Institute for Nuclear Research, Dubna. Translated from Problemy Fiziki Élementarnykh Chastits i Atomnogo Yadra, Vol. 1, No. 2, pp. 547-583, 1971.

TABLE 1

$Q=0$	$Q=Q_p$	$Q=Q_n$	$Q=Q_e$
$\gamma\,(p+p\to p+p+\gamma)$	p	n	e^-
$\pi^0\,(p+p\to p+p+\pi^0)$	$\Sigma^+\,(\Sigma^+\to p+\pi^0)$	$\Lambda^0\,(\Lambda^0\to n+\pi^0)$	$\mu^-\,(\mu^-\to e^-+$ $+\nu+\tilde{\nu})$
$K_1^0\,(K_1^0\to 2\pi^0)$	—	$\Sigma^0\,(\Sigma^0\to\Lambda^0+\gamma)$	—
$K_2^0\,(K_2^0\to\pi^++\pi^-+$ $+\pi^0)$	—	$\Xi^0\,(\Xi^0\to\Lambda^0+\pi^0)$	—

1. Electric Charge of Neutron

The question of the possession of an electric charge by the neutron is closely linked with a more general question: Why are the charges of all elementary particles equal to either $\pm Q_e$, or zero? The neutron is usually regarded as an electrically neutral particle, but there is no theoretical barrier to its having a small charge, and the experimental detection of such a charge would be extremely important for theory.

In modern elementary particle theory the laws of conservation of electric, baryonic, and leptonic charges play a very important role. They are absolute laws, i.e., they are valid for all three types of interaction of elementary particles (strong, electromagnetic, weak). They have been experimentally confirmed with very high accuracy and, together with the laws of conservation of energy, momentum, and angular momentum, govern processes among elementary particles. The essence of these three conservation laws is that particles have three independent sets of numbers Q_i, B_i, L_i (electric, baryonic, and leptonic charge) which satisfy the following relationships:

$$\left.\begin{aligned}\sum_i Q_i &= \text{const in time},\\ \sum_i B_i &= \text{const in time},\\ \sum_i L_i &= \text{const in time}.\end{aligned}\right\} \qquad (1)$$

It can be shown [1, 2] that the application of the law of conservation of electric charge in conjunction with the laws of conservation of baryonic and leptonic charges to known elementary-particle reactions does not enable us to determine the relationship between the electric charges of all elementary particles. For instance, the absence of the reaction $p\to e^+ + \pi^0$ and other similar reactions owing to conservation of baryonic charge means that the charge Q_p of the proton is indeterminate relative to the positron charge Q_e. It does not necessarily follow from the law of conservation of electric charge in conjunction with the laws of conservation of baryonic and leptonic charges that the electric charges of the proton and electron are equal in absolute magnitude, and that the neutron charge is zero.

Table 1 gives four sets of particles with electric charges which are equal owing to the existence of the corresponding reactions.

It is clear that even if the scale of electric charge is fixed by measurement of Q_e, the values of Q_p and Q_n are still indeterminate. Thus, the question of the electric charge of the neutron will have to be settled experimentally.

All the experiments aimed at detecting the neutron charge can be divided into direct and indirect experiments. The direct experiments include experiments on the ionization of gases by neutrons and electrostatic deflection of a beam of very slow neutrons. The earliest experiments (Dee [3]) to detect ionization of gases by neutrons led to the estimate $Q_n < |Q_e|/700$. Shapiro and Éstulin [4] attempted to detect deflection of a beam of thermal neutrons in a homogeneous electrostatic field and obtained an estimate $Q_n < 6\cdot 10^{-12}|Q_e|$. The indirect experiments include attempts to detect the charges of un-ionized atoms and molecules [5-7]. The most accurate investigation, by King [5], gave upper limits for the charges of H2, D2, and SF_6 molecules. The author used a method in which the charge of a macroscopic volume of gas was measured after it had been freed from ions and electrons.

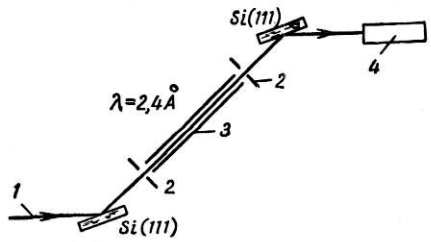

Fig. 1

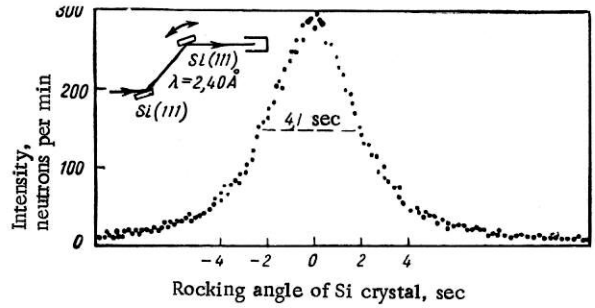

Fig. 2

Fig. 1. Schematic diagram of double-crystal spectrometer and electrostatic deflecting system: 1) Neutron beam; 2) 1.5-mm slit; 3) electrostatic deflecting plates; 4) detector.

Fig. 2. Neutron intensity as function of angular orientation of second crystal.

If one assumes that $Q_{atom}=Z\Delta Q+NQ_n$, where $\Delta Q=|Q_e|-|Q_p|$, Q_n can be estimated independently of ΔQ from the estimates of $Q(H_2)$ and $Q(D_2)$. This procedure gives $Q_n<3\cdot10^{-20}|Q_e|$. If it is assumed that $\Delta Q=Q_n$, the estimate of $Q(SF_6)$ gives $Q_n<2\cdot10^{-22}|Q_e|$.

The indirect estimates are much more accurate than the direct data. Nevertheless, the latter must be regarded as more reliable, since it is quite possible that when particles combine to form an atom they may have their charge altered in some way. A recent accurate direct experiment is that of Shull, Billman, and Wedgewood [8]. The authors managed to attain extremely high angular sensitivity of the instrument by using two successive Bragg reflections from two perfect silicon crystals. A diagram of the apparatus is shown in Fig. 1, and the curve illustrating its angular sensitivity is shown in Fig. 2. The results of the measurement are given in Fig. 3. Treatment by the least squares method gave $Q_n=(-1.9\pm3.7)\cdot10^{-18}|Q_e|$

Estimates of $Q_n=\Delta Q$ can also be obtained from cosmological considerations. Such estimates were made in [9], in particular. A simple consideration of the balance of gravitational attraction and electrostatic repulsion, which ensures the existence of macromatter, leads to $Q_n<10^{-18}|Q_e|$, and a charge of $2\cdot10^{-18}\,Q_e$ is sufficient to account for the observed expansion of the universe within the framework of Newtonian mechanics.

It was suggested in [10] that the magnetic fields of stars and planets might be due to rotation of weakly charged atoms around a polar axis. It follows from these considerations that Q_n must be of the order of $2\cdot10^{-19}\,Q_e$.

A cosmological approach to elementary particle theory has recently been developed [11]. Elementary particles can be regarded in principle as almost closed universes. It is known that a closed world must be electrically neutral, and its total mass must be zero [12]. If an electric charge ε is introduced into such a world, this world will no longer be closed. Its mass will differ from zero and its minimum value will be $m=\varepsilon/\sqrt{\varkappa}$, where $\varkappa$ is the gravitational constant.* If the neutron is considered from this viewpoint, its possible electric charge is $Q_n\leqslant m\sqrt{\varkappa}\sim10^{-18}|Q_e|$, which is very close to the estimates given above. Thus, it would be very desirable to have direct experiments aimed at detecting an electric charge of the neutron at the $10^{-19}|Q_e|$ level.

We note also that the detection of a small neutron charge would mean that the conservation of baryons would follow from the conservation of electric charge [2].

2. Electric Dipole Moment (EDM) of Neutron†

The discovery of CP violation‡ in K°-meson decays removed the theoretical barrier to the possession of an EDM by elementary particles, particularly the neutron. In its transformation properties the EDM of a particle is a polar vector directed along the spin (axial vector) of the particle and hence, as a result of

*A similar formula for any body of mass m can be derived from five-dimensional field theory [13].

†In this section we consider the question of the natural electric dipole moment of the neutron. For the induced EDM see below.

‡Or T violation in view of the well-known CPT theorem.

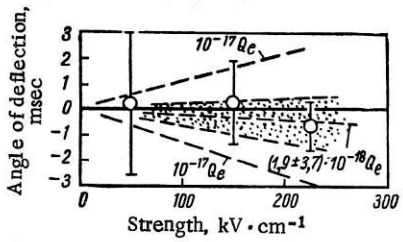

Fig. 3

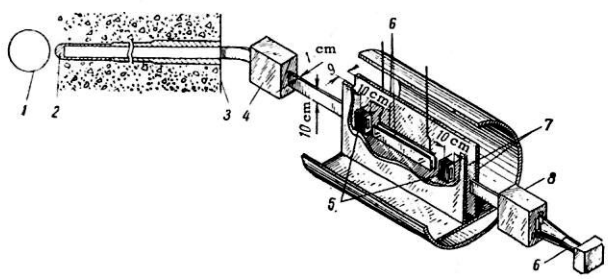

Fig. 4

Fig. 3. Angular deflection of neutron beam by electrostatic field.

Fig. 4. Schematic diagram of Oak Ridge National Laboratory instrument: 1) reactor core; 2) heavy-water moderator; 3) reactor shield; 4) polarizer (Co-Fe mirror); 5) rf coil; 6) electrostatic plates; 7) field magnet pole pieces; 8) analyzer (Co-Fe mirror).

operation of time reversal (reversal of direction of all velocities and replacement of initial state by final state), the relative directions of the EDM and the spin are altered (if the spin and EDM are parallel they become antiparallel). If T invariance exists, the direct and time-reversed states are equally likely and, hence, the observed value of the EDM will be zero [14].

Since numerous searches for violation of T invariance in other processes besides K°-meson decay have been unsuccessful, the detection of an EDM in the neutron, or in any other elementary particle, would be direct evidence of the nonuniversality of the T-invariance principle.

Two experimental methods have been used so far in the search for the neutron EDM. One of these methods – Rabi's magnetic resonance method – was used in 1957 by Smith, Purcell, and Ramsey [15]. They found that the neutron EDM divided by the electron charge $(d_n/e) < 5 \cdot 10^{-20}$ cm. In 1965–1967, as a result of the discovery of the decay of the K_2° meson into two charged pions, attempts to detect a neutron EDM were renewed [16, 17]. In this new experiment a beam of very slow neutrons (mean velocity 60 m/sec) obtained by means of a bent neutron-conducting tube was used. The neutron beam was subjected to the action of a steady magnetic field H_0 and a strong electrostatic field E which could be either parallel ($E\uparrow\uparrow$) or antiparallel ($E\uparrow\downarrow$), to the field H_0. A weak alternating field H_1 with frequency ω was applied perpendicular to the field H_0. The resonance frequency in this case is

$$\omega_0 = \frac{1}{\hbar I}(\mu_n H_0 \pm d_n E), \tag{2}$$

where I is the neutron spin and μ_n is its magnetic moment. The change in resonance frequency on reversal of the electrostatic field is

$$\Delta\omega_0 = \frac{2d_n E}{\hbar I}. \tag{3}$$

When the frequency ω approaches ω_0 there is a resonance change in the spin orientation, accompanied by a sharp change in the intensity of the detected particle beam. The neutron EDM can be determined from the following relationship:

$$d_n = \frac{\hbar}{2} \cdot \frac{\Delta N}{(E_{\uparrow\uparrow} + E_{\uparrow\downarrow}) \frac{dN}{d\nu_{res}}}, \tag{4}$$

where ΔN is the change in the count rate due to the change in the electric field from $E_{\uparrow\uparrow}$ to $E_{\uparrow\downarrow}$; $dN/d\nu_{res}$ is the derivative of the count rate with respect to the alternating field frequency.

The sensitivity of the instrument can be increased by increasing the electric field, or by increasing the steepness of the resonance curve. Since the steepness depends on the resonance line width, and the latter, in turn, is limited by the uncertainty relationship, then it is better to increase the transit time of the neutron through the instrument.

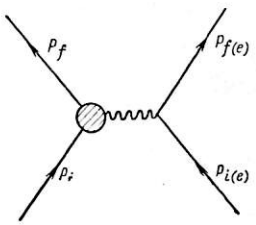

Fig. 5. Feynman diagram for electron scattering by proton in e^2 approximation.

Figure 4 shows a schematic diagram of the Oak Ridge National Laboratory instrument. With E=120 kV/cm and neutron transit time $\tau = 8 \cdot 10^{-3}$ sec, the value obtained in [17] for the neutron EDM was

$$(d_n/e) = (0.02 \pm 0.85) \cdot 10^{-22} \text{ cm}.$$

At the Vienna conference in September, 1968 [18] a new value was reported for the EDM:

$$(d_n/e) = (0.2 \pm 0.2) \cdot 10^{-22} \text{ cm}. \quad (5)$$

The second method was used in the Brookhaven Laboratory [19]. In the presence of an EDM the neutron undergoes an additional interaction with the intraatomic Coulomb field. The corresponding amplitude in the Born approximation has the form

$$b'' = i\, d_n \frac{Ze(1-f)}{\hbar} \cdot \frac{\operatorname{cosec}\theta}{v} (\mathbf{pn}), \quad (6)$$

where Ze is the nuclear charge; $1-f$ is an electronic screening factor; f is the charge distribution form factor; v is the neutron velocity; 2θ is the scattering angle; p is the unit neutron polarization vector, n is the unit scattering vector;

$$\mathbf{n} = \frac{1}{2k \sin\theta} (\mathbf{k} - \mathbf{k}_0), \quad (7)$$

where k and k_0 are the wave vectors before and after collision. The amplitude of (6) is imaginary and maximum when vector p is parallel to n and has its sign changed when the sign of the neutron polarization is reversed. The neutron scattering intensity is

$$\mathcal{J} \sim b^2 + (b' + b'')^2, \quad (8)$$

where b+ib' is the nuclear scattering amplitude.

Shull and Nathans in their experiment tried to detect a change in intensity when the neutron polarization was reversed. Since the relative change in intensity is

$$\frac{\Delta\mathcal{J}}{\mathcal{J}} = \frac{4b'b''}{b^2 + b'^2}, \quad (9)$$

it is better to make the measurements on nuclei with small b. They used in their experiment a CdS single crystal, the intensity of reflection of neutrons from the (004) plane of which depends on the difference in the coherent scattering amplitudes of Cd and S:

$$\mathcal{J} \sim |a_{Cd} - a_S|^2, \quad (10)$$

$a_{Cd} = (3.8 + i\,1,\ 2)$ F and $a_S = 3.1$ F. About $4 \cdot 10^8$ neutrons were counted in the experiment over three months. Special measures were taken to compensate the effects of Schwinger scattering, i.e., scattering due to interaction of the magnetic moment of the moving neutron with the Coulomb field of the nucleus. The amplitude of this scattering is also imaginary, but it becomes zero if the polarization vector is exactly parallel to the scattering vector. The final result of the experiment was

$$\left(\frac{d_n}{e}\right) = (+2.4 \pm 3.9) \cdot 10^{-22} \text{ cm}.$$

Theoretical estimates of the neutron EDM are extremely diverse and, according to them, the neutron EDM lies in the range $10^{-19} > d_n/e > 10^{-31}$ cm. The estimates in the region of 10^{-22} cm are based on the assumption of T violation in weak interactions. From this viewpoint it is very desirable to increase the sensitivity of EDM measurements by one or two orders. Work in this direction is being carried out at Oak Ridge and Brookhaven. A very promising way of increasing the sensitivity of the first method is to use ultracold neutrons, which increases the residence time of particles in the instrument [21]. The second method can be improved by the use of single crystals with a very small coherent scattering amplitude, particularly a mixture of tungsten isotopes enriched with tungsten-186. With an appropriate concentration of W186 the coherent scattering amplitude of such a mixture may even be zero [20].

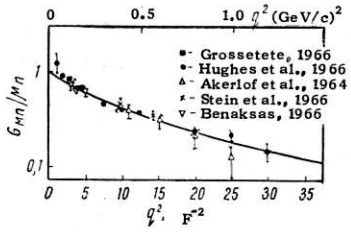

Fig. 6

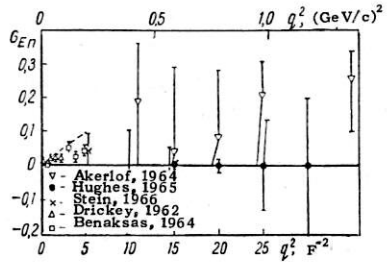

Fig. 7

Fig. 6. Experimental relationship between magnetic form factor G_{Mn}/μ_n and q^2. Curve calculated from formula (23).

Fig. 7. Experimental relationship between G_{En} and q^2.

3. Electromagnetic Structure of Neutron

Electromagnetic Form Factors of Neutron. The properties and structure of any elementary particle are closely related to the properties of other particles. This is due to the existence, for instance, of a cloud of virtual particles around the real neutron. The particles are responsible for the interaction between the neutron and other particles. Although the virtual particles themselves are unobservable in principle, all the effects which they produce are real, like the nuclear forces engendered by the exchange of virtual mesons.

The characteristic dimensions of the cloud of virtual particles depend on their mass. Thus, in order of magnitude the radius of the π-meson cloud is $r_\pi \sim \hbar/m_\pi c$, where m_π is the π-meson mass; that of the K-meson cloud is $r_k \sim \hbar/m_k c$, where m_k is the K-meson mass; and so on. Our present knowledge of the K-mesonic and other deeper shells of the neutron is very slight. We know a little only about the pion cloud.

The electromagnetic structure of the neutron (or of a nucleon in general) is revealed by the interaction of any charged particle with it (e.g., by the scattering of electrons or muons on the nucleon, etc.). This question has been dealt with most fully for the case of electron scattering on nucleons [22]. The laws of electromagnetic interaction are fairly well known and, hence, information regarding nucleon structure can be derived from scattering data. The scattering cross section is first calculated for a point nucleus; electrostatic interaction and the interaction with the normal and anomalous magnetic moments of the particle are neglected. This cross section is then used for calculation of scattering on an extended nucleon consisting of many particles by summation of the waves scattered by each particle. The method employed here is well known from x-ray scattering theory, but in the case of x-ray scattering one is dealing with ordered scattering centers in a crystal lattice, whereas in the case of the nucleon the density distribution is regarded as irregular. Hence, the sum over the different partial scattering amplitudes is replaced by an integral, which is called the form factor.

A rigorous theoretical examination of this question, satisfying the requirements of Lorentz and gradient invariance in the approximation corresponding to the Feynman diagram (Fig. 5), indicates that the representation of the electromagnetic structure of a nucleon requires two form factors – F_1 and F_2 – which are functions of the square of the transmitted four-momentum q*:

$$q^2 = (p_f - p_i)^2 = (p_{f(e)} - p_{i(e)})^2, \tag{11}$$

where p_i, p_f, $p_{i(e)}$, and $p_{f(e)}$ are the initial and final four momenta of the proton and electron.

It can be shown [23] that when $E \gg m$,† where E is the energy and m the mass of the electron,

$$q^2 = -\frac{(2E\sin\theta/2)^2}{1+2\frac{E}{M}\sin^2\frac{\theta}{2}}. \tag{12}$$

where M is the nucleon mass, and θ the electron scattering angle. For the case described by the Feynman diagram (Fig. 5), $q^2 < 0$ (spacelike values of q).

*We recall that the spatial components of the four-momentum vector are the same as the particle momentum p, while the time component is i E/cj, where E is the particle energy.

†A system of units in which $\hbar = c = 1$ is used.

The Dirac form factor $F_1(q^2)$ describes the spatial distribution of nucleon charge and the associated Dirac magnetic moment. The Pauli form factor $F_2(q^2)$ is related to the spatial distribution of the anomalous magnetic moment. The form factors represent the cumulative result of all the effects produced by any number of virtual particles. This means in diagram terms (Fig. 5) that the interactions occurring at the nucleon-photon vertex are not detailed. The hatched region represents only the ultimate result. In the limiting case of low energies (small momentum transfers), when the nonrelativistic approximation is valid, the form factors represent the Fourier transform of the spatial distribution of electric charge $\rho(r)$ and magnetic moment m(r). For instance, in the case of a spherically symmetrical charged particle $F_1(q)$ is given by:

$$F_1(q) = \frac{4\pi}{qe}\int_0^\infty \rho(r)\sin(qr)\,r\,dr, \tag{13}$$

where $\rho(r)$ is the electric charge distribution density. We find from formula (13) that

$$\rho(r) = \frac{e}{2\pi^2 r}\int_0^\infty F(q)\sin(qr)\,q\,dq. \tag{14}$$

It follows from (13) that $F_1(0)=1$. Similarly, $F_2(0)=1$. A point particle with charge e and total magnetic moment $e\hbar/2Mc+\mu_0$, where $\mu_0=\varkappa e\hbar/2Mc$, is a particle for which F_1 and F_2 are independent of q and equal to 1. The particle has an electromagnetic structure only in the case where $F_1(q^2)$ and $F_2(q^2)$ are not constant. This statement is an exact definition of the electromagnetic structure of a particle for all q^2 [17].

If $\rho(r)$ and m(r) are known, the rms electric and magnetic radii of the particle can be determined:

$$\langle r_e^2\rangle = \frac{\int r^2\rho(r)\,d^3r}{\int \rho(r)\,d^3r} = \frac{6F_1'(q^2)_{q^2=0}}{F_1(0)}; \tag{15}$$

$$\langle r_m^2\rangle = \frac{\int r^2 m(r)\,d^3r}{\int \rho(r)\,d^3r} = \frac{6F_2'(q^2)_{q^2=0}}{F_2(0)}. \tag{16}$$

In the case of the neutron $F_{1,n}=0$ and the rms radius is given by

$$\langle r_e^2\rangle_n = \frac{6F'_{1,n}(q^2)_{q^2=0}}{F_{1,p}(0)} = 6F'_{1,n}(q^2)_{q^2=0}. \tag{17}$$

At small q^2 functions F can be expanded in a series:

$$F_{1,2}(q^2) \approx F_{1,2}(0) + q^2F'_{1,2}(q^2)_{q^2=0} + \ldots = F_{1,2}(0)\left(1+\frac{1}{6}q^2\langle r^2\rangle_{1,2}+\ldots\right). \tag{18}$$

It is clear from (18) that when $q^2\to 0$ the rms radius determines the slope of the form factor and in this sense can serve as a characteristic of the form factor, if the latter is not a rapidly varying function of q^2. Otherwise the value $\langle r^2\rangle$ will not be related to the general behavior of the form factor. From (17) and (18) and for the case of a neutron we obtain

$$F_{1,n}(q^2) \approx q^2\frac{1}{6}\langle r_e^2\rangle_n + \ldots; \tag{19}$$

$$F_{2,n}(q^2) \approx F_{2,n}(0)\left(1+\frac{q^2}{6}\langle r_m^2\rangle_n + \ldots\right) = 1 + \frac{q^2}{6}\langle r_m^2\rangle_n. \tag{20}$$

As already mentioned, each of the form factors F_1 and F_2 does not describe merely the distribution of charge or magnetic moment. There is a coordinate system, however, in which the combinations of form factors F_1 and F_2 correspond very accurately with the distribution of electric charge and magnetic moment. The new form factors are expressed in terms of F_1 and F_2 as follows [24]:

the charge form factor

$$G_E(q^2) = F_1(q^2) + \frac{q^2}{4M^2}\varkappa F_2(q^2), \tag{21}$$

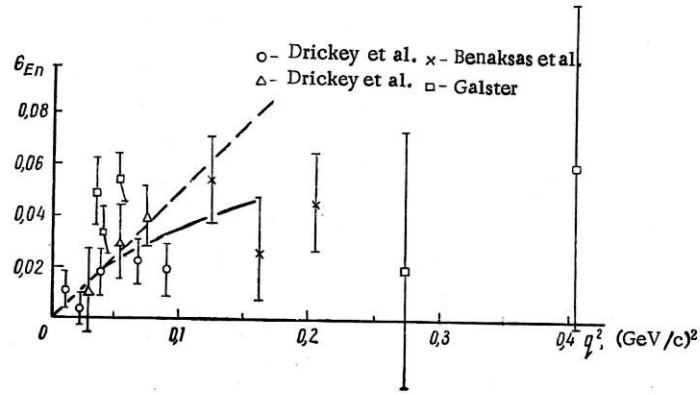

Fig. 8. Experimental relationship between neutron charge for form factor G_{En} and q^2 for $q^2 \leq 0.4$ (GeV/c)².

the magnetic form factor

$$G_M(q^2) = F_1(q^2) + \varkappa F_2(q^2). \tag{22}$$

The corresponding coordinate system is specified by the requirement that the spatial components of the vector $p_i + p_f$ are equal to zero. In such a system the three momenta of the initial and final protons are equal and opposite in direction, and the energies corresponding to this case are equal. The introduction of G_E and G_M also makes the treatment of the experimental data easier.

The bulk of information on G_E and G_M at present has been obtained from data for electron scattering on protons and deuterons. Figures 6 and 7 show the experimental values of G_{Mn}/μ_n and G_{En} reported at the Stanford Conference in 1967 [25]. It was experimentally established that G_{Ep}, G_{Mp}, and G_{Mn} are connected by the following relationship:

$$G_{Ep}(q^2) = \frac{G_{Mp}(q^2)}{\mu_p} = \frac{G_{Mn}(q^2)}{\mu_n} \approx \frac{1}{(1+q^2/0.71)^2}. \tag{23}$$

The results of recent, very accurate measurements made in Bonn University [26] reveal slight deviations from this relationship.

Figure 8 shows the experimental G_{En} data for $q^2 \leq 0.4$ (GeV/c)². The broken line – slope at $q^2=0$ – was obtained from ne-interaction data. The solid curve is the result of dispersion calculations [27]. Since the neutron form factor values were obtained from an analysis of experiments on electron scattering on deuterons, and there is no strict relativistic theory for the deuteron, these values are not reliable enough. This applies particularly to G_{En} at low q^2. The information about $(\partial G_{En}/\partial q^2)_{q^2=0}$ obtained from ne-interaction experiments is more reliable (see section "Neutron-Electron Interaction").

Polarizability of Neutron. The concept of polarizability of nucleons was introduced in connection with photon scattering and pion photoproduction on nucleons [28, 29], and with neutron scattering on heavy nuclei [30, 31]. Along with the charge, magnetic, and other moments, the polarizability (electric and magnetic) is a characteristic of the particle which has to be introduced for a complete description of the interaction of elementary particles. The polarizability is an index of the deformation of the meson cloud of the particle due to electric and magnetic fields. It is zero if the particle has a rigid, nondeformable structure, or is a point particle. It is rather difficult to determine the polarizability of a nucleon experimentally. Some measurements have been made in the case of the proton. Its electric polarizability has been determined [32]. In the case of the neutron all we can say at present is that there are experimental estimates of quantities of interest. These estimates have been obtained from experiments with photons and neutrons.

Photon Scattering. Scattering of photons by particles with spin 1/2 and an anomalous magnetic moment was examined in [28, 29, 33-38]. In the low-frequency region, i.e., when $\omega \ll m$, where ω is the photon frequency, and m is the pion mass, the obvious approach is to expand the scattering amplitude in terms of the photon frequency. In [28, 33, 34] linear frequency terms were considered. It was shown that in this case the scattering can be described if the charge, mass, and anomalous magnetic moment are

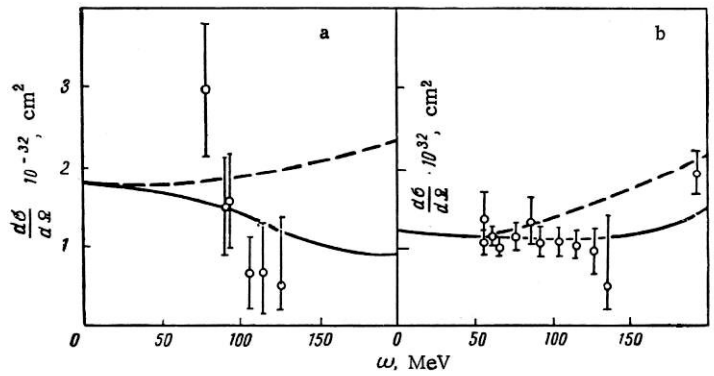

Fig. 9. Cross section for elastic scattering of photons on protons at angles of 45° (a) and 90° (b) as functions of energy. The continuous curve represents the results of calculation with $\alpha_p = 0.9 \cdot 10^{-42}$ cm^3 $\beta_p = 0.2 \cdot 10^{-42}$ cm^3. The dashed curve represents the results of calculation with $\alpha_p = \beta_p = 0$.

known. This description, however, is not exhaustive. In [28] the possible implication of intermediate states corresponding to high excitation of the nucleon in low-energy processes was considered. The absorption of a photon by a nucleon leads to the induction of electric and magnetic moments in the nucleon and their subsequent emission. A similar effect is known in optics under the name of Rayleigh scattering. The Rayleigh scattering amplitude is proportional to the square of the γ-ray frequency. It was shown that at energies below the pion production threshold a similar consideration necessitates the introduction of two new parameters – the α and β coefficients of the electric and magnetic polarizability of a nucleon.

There have been many theoretical investigations devoted to the definition of the concept of polarizability in photon scattering and the theory of the Compton effect. It has been shown that in a consideration of low-energy photon scattering on a system with spin 1/2, accurate to terms containing the cube of the photon frequency, the formula for the scattering amplitude contains another three terms in addition to the charge, mass, and anomalous magnetic moment. These are α, β, and $\langle r_e^2 \rangle$, the rms radius of the charge distribution. A fuller review of these investigations can be found in [39].

The values of α_p and β_p can be obtained from experiments on the elastic scattering of photons on protons at energies below the pion production threshold. These experiments were analyzed in [40]. The results of the analysis give the following values for the proton (Fig. 9): $\alpha_p = (0.9 \pm 0.2)\ 10^{-42}$ cm^3, $\beta_p = (0.2 \pm 0.2)\ 10^{-42}$ cm^3.

It should be noted that inclusion of terms higher than the third order in the expansion of the scattering amplitude in terms of the frequency can slightly alter the value of α_p. If their effect is to be excluded, the measurements must be made at γ-ray energies of the order of 10-20 MeV. This involves great difficulties, however, owing to the great reduction of the effect with energy reduction.

It is much more difficult to evaluate the polarizability of the neutron, since it is impossible to obtain direct experimental data on photon scattering by neutrons. It will be possible in the future to carry out a direct experiment in which neutrons will collide with a powerful laser beam, but in the meantime the neutron polarizability has to be estimated from information obtained from Compton-effect experiments, particularly on the deuteron. The difficulties in the analysis of these experiments; as in the analysis of experiments on electron scattering on deuterons, are due primarily to the lack of a strict relativistic theory of the deuteron. The fact that the neutron is in motion in the deuteron must be taken into account. At the present stage of relativistic deuteron theory the problem of the effect of motion can be solved only approximately. Several assumptions have to be made and these ultimately reduce the reliability of the results.

The analysis of deuteron Compton-effect data is usually performed within the framework of the impulse approximation [41]. In this approximation the scattering amplitude on the deuteron is considered to be equal to the sum of the scattering amplitudes on the free proton and neutron, and the momentum distribution of these particles is taken to be the same as in the deuteron. However, as was shown in [29, 42, 43], the experimental data for photon scattering on deuterons [44, 45] do not fit into the framework of the

impulse approximation. Photodisintegration of the deuteron has a pronounced effect on the scattering amplitude of the considered process in the energy range 50-100 MeV. This inelastic process, together with pion photoproduction at high energies, makes the impulse approximation invalid for the examination of the Compton effect on the deuteron in a wide energy range. The ultimate result is that no reliable conclusions regarding the polarizability of the neutron can be derived from experiments on photon scattering on deuterons.

In a recent investigation [42] the authors examined experimental deuteron Compton-effect data and came to the conclusion that the electric polarizability of the deuteron cannot exceed the corresponding value for the proton by more than 40%. This conclusion, however, was based on the impulse approximation and, as the authors themselves state, the consideration of some exchange effects can lead to a much higher value of α_n.

In [29] attention was given to the fact that a study of $\gamma+d\to d+\gamma$ and $\gamma+He^4\to He^4+\gamma$ processes can simplify the interpretation of the experimental data. As regards the first process, it is evident that at energies of the order of several tens of megaelectron-volts it is difficult to separate from the $\gamma+d\to p+n+\gamma$ process, while the polarizability is proportional to the square of the photon frequency, and at very low photon energies the effect is small. The possibility of evaluating α_n from an investigation of the $\gamma+He^4\to He^4+\gamma$ reaction was considered in [37]. In this case the contribution of inelastic processes to the scattering amplitude is much less than in the case of the deuteron, since the helium photodisintegration threshold is fairly high ($E\sim 20$ MeV). As was shown in [37], photon scattering on helium at an angle of 90° can be measured and the value of $\bar{\alpha}$ obtained from:

$$\bar{\alpha}=\alpha+\frac{1}{3}\left(\frac{e^2}{M}\right)\langle r_e^2\rangle, \tag{24}$$

where $\langle r_e^2\rangle$ is the rms radius of helium determined from experiments on $e-He^4$ scattering, and the helium polarizability $\alpha=\alpha_N+2\alpha_p+2\alpha_n$. The value of α_N can be determined from helium photodisintegration experiments by using the expression known from dispersion relations:

$$\alpha_N=\frac{1}{2\pi^2}\int\frac{\sigma_{E1}\,d\omega}{\omega^2}, \tag{25}$$

where σ_{E_1} is the total dipole absorption cross section (with meson photoproduction neglected). The integral (25) can be evaluated by replacing σ_{E_1} by σ_{tot}. This gives $\alpha_N=(70\pm4)\cdot10^{-42}$ cm^3. The accuracy of this evaluation determines the upper limit of α_n. This method can be used to determine the value of α_n, if it is more than, or of the order of, $5\cdot10^{-42}$ cm^3. There have not yet been any experiments on photon scattering on helium.

An indirect estimate of the neutron polarizability can be obtained from meson photoproduction data [29, 38]: $\gamma+p\to\pi^++n$, $\gamma+n\to\pi^-+p$. From dispersion relations we have [38]:

$$\alpha=\frac{1}{2\pi^2}\int_{\omega_t}^{\infty}\frac{d\omega}{\omega^2}\left\{|E_1|^2+2|E_3|^2+\frac{1}{3}|E_2|^2-\frac{1}{6}|M_2|^2\right\}; \tag{26}$$

$$\beta=\frac{1}{2\pi^2}\int_{\omega_t}^{\infty}\frac{d\omega}{\omega^2}\left\{|M_1|^2+2|M_3|^2+\frac{1}{3}|M_2|^2-\frac{1}{6}|E_2|^2\right\}, \tag{27}$$

where E_i and M_i are the partial amplitudes of pion production on the nucleon (electric and magnetic types). It is known from experiments on pion photoproduction on protons and deuterons that the ratio of the cross section $\sigma_\pi/\sigma_{\pi+}$ near the threshold is ~1.3 [45]. Since electric dipole pion production dominates at these energies, it can be assumed that $|E_1^-|^2\sim1.3|E_1^+|^2$. Hence, taking into account the value of α_p, we can obtain for the neutron $\alpha_n\sim1.2\cdot10^{-42}$ cm^3. A similar value was found in [46]. The true value of α_n is evidently close to the obtained values. There have been no experimental estimates of β_n.

Neutron Scattering by Heavy Nuclei. An upper estimate of the electric polarizability of the neutron can be obtained by investigating neutron scattering by heavy nuclei. The concept of electric polarizability of the neutron was introduced in connection with the question of neutron scattering in [30, 31]. In the Hamiltonian for neutron-nucleus interaction there appears an additional term of the form $\frac{1}{2}\alpha_nE^2$, where

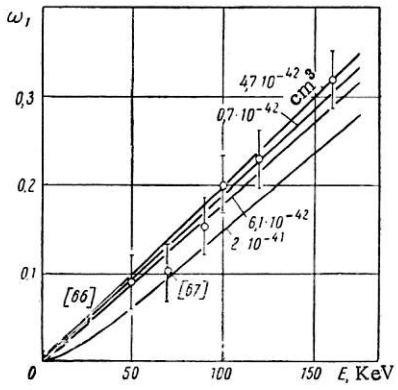

Fig. 10. ω_1 as function of neutron energy. Curves calculated from formulas (31) and (32) with fixed $\alpha = 1.91 \cdot 10^{-3}$ and indicated values of α_n.

E is the electric field of the nucleus. In [31] the amplitude of polarization scattering of the neutron in the Coulomb field of the nucleus was calculated in the Born approximation:

$$f(\theta) = \frac{M\alpha_n}{2R}\left(\frac{Ze}{\hbar}\right)^2 KR\left(\frac{\sin KR}{K^2R^2} + \frac{\cos KR}{KR} + \sin KR\right) \qquad (28)$$

where $K = (2\sin\theta/2)/\lambda$; R is the radius of the nucleus; M is the reduced neutron mass.

On the assumption that the energy of nuclear interaction is independent of the spin the following expression was obtained for the differential cross section for elastic scattering of unpolarized neutrons:

$$\frac{d\sigma}{d\Omega} = |f_0(\theta)|^2 + \frac{1}{4}\varkappa_n^2\left(\frac{\hbar}{Mc}\right)^2\left(\frac{Ze^2}{\hbar c}\right)^2 \operatorname{ctg}^2\frac{\theta}{2} + 2\,\mathrm{Re} f_0(\theta) f(\theta) + f^2(\theta), \qquad (29)$$

where $f_0(\theta)$ is the nuclear scattering amplitude. The second term of expression (29) represents the Schwinger scattering resulting from the interaction of the neutron magnetic moment $\mu_n = \varkappa_n e\hbar/2Mc$ with the Coulomb field of the nucleus. Since polarization scattering is due to long-range forces the effects caused by them at neutron energies of the order of several megaelectron-volts must be sought at small angles ($< 10°$). Besides the effect due to neutron polarizability, there will also be Schwinger scattering in the small-angle region, but the effect of this can be taken into account sufficiently accurately by calculation.

The main difficulty in interpretation of the experimental data lies in the assessment of nuclear interaction. Since there is no appropriate rigorous theory, the consideration of the effect of nuclear interaction necessitates model ideas of a different kind. In a first approximation nuclear scattering at angles $< 10°$ at energies above 1 MeV can be regarded as isotropic. In fact, a neutron which has undergone interaction in a region of radius R (radius of nucleus) has an uncertainty in momentum of $\Delta p \sim \hbar/R$, which leads to uncertainty in the scattering angle θ: $\tan\theta = \Delta p/p \sim \hbar/pR = 1/kR$. If $R \sim 10^{-12}$ cm, the kinetic energy of the neutron $E_n \sim 2$ MeV, then $\tan\theta \sim 1/3$ and $\theta \sim 18°$, i.e., down to angles of 20° (or less) scattering is equally probable. In the first investigations of low-angle scattering of neutrons with energy of the order of several megaelectron volts [47-49], the results of the experiment after correction for Schwinger scattering were compared either with the relationship for nuclear scattering of the form $\sigma(\theta) = A + B\cos\theta$ [47, 48] or with the diffraction formula [49]. In both cases the behavior of the differential cross section in the low-angle region showed deviations from the above relationships for uranium, thorium, and plutonium. There were no deviations in the case of lighter nuclei. If these deviations are attributed to the effect of the electric polarizability of the neutron, the value of α_n obtained ($\alpha_n \sim 10^{-40}$ cm^3) is too high, which contradicts not only the experimental value of the proton electric polarizability, from which α_n cannot differ too greatly, but also a whole series of theoretical calculations made for nucleons [50-54].

In later experimental investigations of low-angle scattering [55-60] covering the neutron energy range from 0.5 to 14 MeV, the results of the measurements were compared with calculations based on the optical model of the nucleus. It is difficult at present to speak of any regularity in the differences between the calculated and experimental value. Nevertheless, the purely classical optical model is not satisfactory for small angles – the inclusion of the long-range potential improves the agreement between calculations and experiment. Anikin came to this conclusion after a thorough analysis of the experimental data of [47-49, 55-60] by using for the computer calculations a program which included a long-range potential of the form $1/r^4$ and which allowed a direct selection of the parameters of the optical model during calculation so that the best agreement with the experimental data for angular scattering distributions and total cross sections could be secured.

In [61-64] attempts were made to include effects capable of causing various kinds of anomalies in the low-angle region, but they were not successful. The presence of uncertainty in calculations of the behavior of the nuclear scattering cross section greatly reduces the accuracy of the upper limit for the neutron electric polarizability derived from the discussed experiments. All that one can say is that $|\alpha_n| < (2\text{-}3)\cdot10^{-40}$ cm^3.

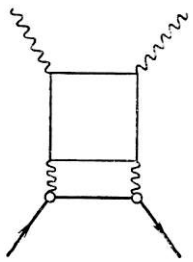

Fig. 11. Scattering due to polarizability of electron-positron cloud of charged particle in Coulomb field.

Another series of experiments from which an upper estimate for α_n can be obtained are experiments on neutron scattering by heavy nuclei in the low-energy region (less than 100 keV) [65, 66]. If the differential scattering cross section is put in the form

$$\sigma(\theta)=\frac{\sigma_0}{4\pi}\left[1+\sum_{l=0}^{\infty}\omega_l P_l(\cos\theta)\right], \tag{30}$$

where σ_0 is the total potential scattering cross section and the well-known approximate relationship $\delta_l \sim (kR)^{2l}$ is used for the scattering phases on the short-range potential of the nucleus, it is easy to show that in the case of purely nuclear interaction the coefficient ω_1 is a linear function of the neutron energy E. If the interference of nuclear scattering and polarization scattering is taken into account ω_1 will contain a term proportional to k, so that

$$\omega_1 = aE + bE^{1/2}, \tag{31}$$

where

$$b=-2.5\times10^{-4}\frac{M^{3/2}e^2}{\hbar^3}\cdot\frac{\alpha_n Z^2}{\sigma_0^{1/2}}. \tag{32}$$

If the energy E in formula (31) is expressed in kiloelectron-volts. Such an analysis was performed in [65] for scattering of neutrons with energies of 50-300 keV on uranium nuclei and led to the estimate $|\alpha_n| < 20 \cdot 10^{-42}$ cm^3. A more suitable region for investigations is the energy region below 50 keV, since in this energy region the nonlinear variation of ω_1 with E is much more appreciable. The authors of [66] carried out experiments on neutron scattering in the energy region 0.6 – 26 keV (time-of-flight method, pulsed reactor). The material chosen for the scatterer was lead, which has no strong neutron resonances in the investigated energy region. This ensures that there is no uncertainty in the analysis due to neglect of the role of resonances. The obtained data were treated by the least-squares method in conjunction with the data of Langsdorf et al. in [67]. This treatment led to the conclusion that with a probability of 70% the value of α_n lies in the following range (Fig. 10): $-4.7\cdot10^{-42}$ cm$^3 \lesssim \alpha_n \lesssim 6.1\cdot10^{-42}$ cm^3. This result is the best direct experimental estimate of α_n so far.

Polarizability of Nucleons due to Nonlinear Electrodynamic Effects. So far we have been dealing with the polarizability of the nucleon due to the cloud of virtual pions surrounding it. The nucleon, however, is always surrounded by a cloud of virtual electron-positron pairs of radius $\hbar/2m_ec \sim 10^{-11}$ cm. This was considered in [68]. As was reported in [68], it is possible that an appreciable role in the scattering of nucleons on nuclei is played by sixth-order diagrams in e with a photon scattering block due to the Coulomb field of the nucleus. The corresponding diagram is shown in Fig. 11. The total coefficient for the quadratic frequency terms in this case can be written in the form [68]

$$\left.\begin{aligned}\alpha_t &\sim \int_{\omega_t}^{\infty}\frac{\sigma_t(\omega)\,d\omega}{\omega^2},\\ \alpha_t &= \alpha_m + \alpha_e,\end{aligned}\right\} \tag{33}$$

where α_m and α_e are the contributions from mesonic and electrodynamic processes.

Because of the special nature of the angular dependence of γp scattering only the mesonic part, i.e., α_m, plays a significant role in large-angle scattering at energies of the order of 50-100 MeV. In the case of small-angle scattering or at very low energies the effect of electron-positron pair production becomes significant. Substituting in (33) the cross section for pair production on the proton we find that $\alpha_{ep}=0.7\cdot10^{-39}$ cm^3. Such a large value could certainly be detected in the case of proton scattering by heavy nuclei. For a similar estimate for the neutron we need to know the cross section for e^+e^- pair production on the neutron. In [68] the cross section for e^+e^- pair production on the anomalous magnetic moment of the neutron was calculated. The results of calculation from formula (33) give $\alpha_{en} \sim 10^{-44}$ cm^3. No neutron or photon experiments have shown such a small value so far.

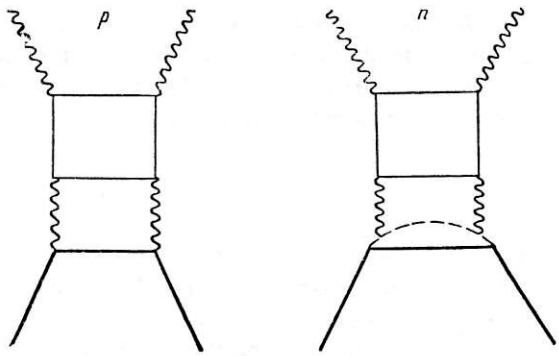

Fig. 12. Scattering due to polarizability of electron-positron cloud of proton and nucleon in Coulomb field.

It was reported in [69] that the main contribution to α_{en} could be made by pair production due to the electrically charged pion cloud, and not to the anomalous magnetic moment of the neutron. Diagrams representing the electromagnetic interactions of nucleons by their polarizability due to the cloud of virtual electron-positron pairs are shown in Fig. 12 for the proton and neutron. The polarizability of the electron-positron cloud in the proton and neutron [70] has the following order:

$$\alpha_{ep} \sim \overline{G}_{Ep} \left(\frac{e^2}{\hbar c}\right) \left(\frac{\hbar}{2m_e c}\right)^3; \tag{34}$$

$$\alpha_{en} \sim \overline{G}_{En} \left(\frac{g^2}{\hbar c}\right) \left(\frac{e^2}{\hbar c}\right) \left(\frac{\hbar}{2m_e c}\right)^3, \tag{35}$$

where $\bar{G}_{Ep}$ and $\bar{G}_{En}$ are the mean values of the charge form factor of the proton and neutron; g is the strong coupling constant. $\bar{G}_{Ep}$ for the proton is known, and the substitution of the values of the constants in [34] gives $\alpha_{Ep} \sim 1.5 \cdot 10^{-39}$ cm^3, which is close to the value obtained from expression (33). The neutron charge form factor, according to the data of [25, 71, 72], in the region of $q^2 = (0-2)f^{-2}$ *does not exceed 0.03-0.05. Hence, the value of α_{en} will be small and can hardly have a significant effect on neutron scattering by heavy nuclei at the considered energies, although more accurate calculations are required for a definitive conclusion, since different values of q^2 make a contribution to the cross section in the case of interaction of the neutron with the Coulomb field of the nucleus. In addition, as was reported in [68], there may be a strong energy dependence at the threshold for pair production by collision of a neutron with the nucleus. It is possible that effects of this kind can cause the anomalous scattering of neutrons by heavy nuclei at small angles at energies of several megaelectron-volts and have no effect in the very low-energy region. At any rate, this question requires further investigation.

Within the frameworks of SU_3 and SU_6, relationships between the electric and magnetic polarizabilities of baryons and mesons [73] can be obtained. The electric polarizabilities of baryons are connected by the relationships:

$$\left.\begin{aligned} &\alpha_p = \alpha_{\Sigma^+}; \quad \alpha_n = \alpha_{\Xi^0}; \quad \alpha_{\Sigma^-} = \alpha_{\Xi^-}; \\ &\alpha_{\Sigma^0} - \alpha_{\Lambda^0} = 1\ (\alpha_{\Lambda^0} - \alpha_n) = \frac{2\sqrt{3}}{3}\ \alpha_{\Sigma^0\Lambda^0}, \end{aligned}\right\} \tag{36}$$

where $\alpha_{\Sigma^0\Lambda^0}$ is the matrix element of two-photon decay

$$\Sigma^0 \to \Lambda^0 + 2\gamma.$$

The baryon magnetic polarizability β satisfies similar relationships.

In [74] relationships between the polarizabilities of baryons and mesons were obtained on the basis of the nonrelativistic quark model of elementary particles possessing SU_6 symmetry. In particular, within the framework of this model $\alpha_p = \alpha_n$, $\beta_p = 1.5 \cdot 10^{-43}$ cm^3, $\beta_n = 1.2 \cdot 10^{-43}$ cm^3.

*The momentum $1f \approx 10^{13}$ cm^{-1} = 197 MeV/c.

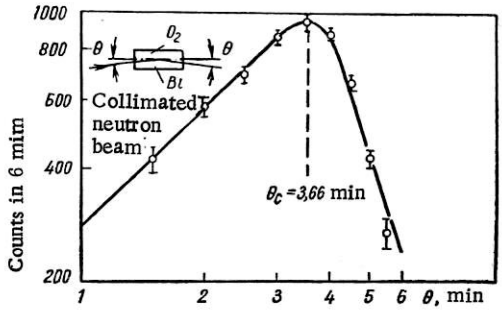

Fig. 13. Setup and results of experiment of Hughes et al. [85, 86].

Thus, electrons and photons are mutually supplementary means of investigating the electromagnetic structure of nucleons. The form factors G_E and G_M, which characterize the distribution of charge and magnetic moment of the nucleon, are determined from electron scattering. Polarizability – the ability of the meson cloud of the nucleon to undergo deformation – is manifested in interaction with photons. There is evidently a close link between the form factors and the polarizability, but this question has not been examined yet.

4. Neutron-Electron (ne) Interaction

Introduction. Since the neutron has a magnetic moment, there is a spin-dependent interaction of the dipole moments of the neutron and electron, and also a velocity-dependent interaction of the magnetic moment of the neutron with the electric field of the moving electron. These interactions, which lead to magnetic scattering of slow neutrons on atoms, are investigated by the techniques of neutron optics: small-angle scattering, diffraction, reflection, etc. [75, 76]. Spin- and velocity-independent interaction of the neutron and electron can occur if the neutron has a spatial electromagnetic structure. In this case there may be regions with non-zero charge density inside the neutron. Any charged particle getting "inside" the neutron will be subjected in this case to the action of electromagnetic forces. Any other charged particle could be taken as the object of investigation in place of the electron. In the case of the proton, however, the nuclear interaction between it and the neutron is not known well enough for us to identify the small electromagnetic contribution. For other particles, μ mesons for instance, such experiments are impossible owing to inadequate experimental technique.

The sought cross section for scattering of the neutron by the electron is eight orders less than the nuclear interaction cross section. Nevertheless, this effect can be detected from the interference between the elastic scattering of slow neutrons by the nucleus and electrons of the atom. The differential cross section for coherent scattering of slow neutrons with wavelength λ of the order of the atomic radius is described (absorption being ignored) by the relationship

$$\sigma(\theta) = \left| a + Zf\left(\frac{\sin\theta}{\lambda}\right) a_{ne} \right|^2, \tag{37}$$

where a is the coherent nuclear scattering amplitude; a_{ne} is the scattering amplitude of the neutron on the electron; $f(\sin\theta/\lambda)$ is the atomic form factor for electrons, which is known from x-ray scattering [77]. Estimates show that the relative magnitude of the additional contribution to the scattering

$$\frac{\Delta\sigma}{\sigma} \approx 2Z\,\Delta f \frac{a_{ne}}{a} \tag{38}$$

is about 1%. An effect of this magnitude can be measured. In neutron physics the ne interaction is usually described by a constant equivalent potential V_0, connected with the scattering amplitude by the expression

$$a_{ne} = \frac{2}{3} \cdot \frac{MR^3}{\hbar^2} V_0. \tag{39}$$

For the radius R of the potential well we take the classical electron radius $e^2/mc^2 = 2.8 \cdot 10^{-13}$ cm. Of course, the potential V_0 is of a purely arbitrary nature, since in this problem the classical electron radius does not play a fundamental role.

Experimental Methods of Determining ne Interaction. Neutron-electron interaction has been investigated by three methods which have now become classical. One of them [78] consists in observing the very small asymmetry of the scattering of thermal neutrons due to the variation of $f(\sin\theta/\lambda)$ with scattering angle. In this and similar experiments the scattering of thermal neutrons with a Maxwellian velocity distribution at angles of 45° and 135° is compared. Effects due to magnetic scattering and molecular diffraction are avoided by using noble gases with filled electron shells, particularly xenon (Z=54), as scatterers.

Table 2

Method	V_0, eV	Literature
Scattering on Xe	(300±5000)	[78]
Total cross section for Pb	Less than 5000	[82]
Total cross section for Bi	—(5300±1000)	[83]
Reflection from O_2-Bi mirror	—(3860±370)	[85, 86]
Scattering on Xe, Kr, Ar	—(4100±1000)	[79]
Measurement of amplitudes of Xe, Kr	—(3900±800)	[80]*
Total cross section for Bi	—(4340±140)	[84]
Scattering on Xe, Kr, Ar, Ne	—(3720±90)	[81]
Reflection from Bi mirror	—(4100±100)	[88]

*The authors used the data of [79].

The values $f(45°)=0.78$ and $f(135°)=0.52$ for thermal neutrons are responsible for the asymmetry of ne scattering, which is superimposed on the strong isotropic nuclear scattering. A correction must be introduced into the measured value of the asymmetry for the different geometric parameters of the detectors and to allow for the assymmetry due to the thermal motion of the gas atoms, which is many times greater than the sought effect. The measurements described in [75] and subsequent more accurate experiments [79, 80] led to a value $V_0=-(3900\pm800)$ eV; the minus sign corresponds to attraction between the neutron and electron. The main fault of experiments of such type is the large value of the correction for the effect due to thermal motion of the gas atoms. The main contribution to the correction comes from neutrons which have a very large wavelength in precisely that region where deviations from a Maxwellian distribution can be expected. This can lead to incorrect calculation of the correction. In the most accurate experiments this correction was determined experimentally from measurements with argon or neon, for which ne scattering is insignificant.

Accurate experiments by the method described in [75] were those carried out [81] in the Argonne National Laboratory in 1965-1966. Xenon, krypton, and argon were used in the experiments. Neon was used to check the calculated correction for asymmetry due to thermal motion of the gas. The magnitude of this correction exceeded the required effect for xenon by a factor of 4, for krypton by a factor of 10, and for argon by a factor of 18. The ne scattering amplitude was determined from the relationship

$$R=1+8\pi\frac{aa_{ne}}{\sigma_s}Z\,\Delta f\,(1+\delta), \tag{40}$$

where $R=\sigma(45°)/\sigma(135°)$ is the measured asymmetry, including a correction for "false" asymmetry; a is the nuclear scattering length; σ_s is the scattering cross section; $\Delta f=\langle f(45°)-f(135°)\rangle$ is the form factor difference averaged over the neutron spectrum,

$$\delta\approx\frac{a_{ne}}{2a\,\Delta f}\langle f^2 45°)-f^2(135°)\rangle-\frac{8\pi aa_{ne}}{\sigma_s}\langle f(135°)\rangle.$$

The value of σ did not exceed 0.01. The values of a for Xe and Kr were obtained by measurement of the critical angles of total reflection of neutrons from the surfaces of liquefied gases. The value of a for Xe was also obtained from experiments on neutron diffraction on XeF_4.

The final result of the experiment was as follows:

$$a_{ne}=(-1.34\pm0.03)\cdot10^{-16}\ \text{cm}\quad\text{or}\quad V_0=(-3720\pm90)\ \text{eV}. \tag{41}$$

The second method of investigating ne interaction was used by Havens, Rainwater, and Rabi [82, 81]. It consists in observing the variation of the total scattering cross section with neutron wavelength in the $\lambda\sim1$ Å region. The nuclear scattering amplitude is constant, whereas the form factor $f(\sin\theta/\lambda)$ is responsible for the variation of the total cross section with λ. In [82, 83] the authors used liquid lead, and then liquid bismuth, as scatterers. They measured the total cross section for liquid bismuth in the range $\lambda=0.3-1.3$ Å. In this wavelength range the change in the form factor due to ne interaction causes a change of 0.1 b in the total cross section. Corrections for other effects must be introduced into the measurements. For instance, the correction for interatomic interference effects is 0.2 b in this wavelength range. A correction has to be introduced for the relative velocity due to thermal motion of the target atoms, and also for the

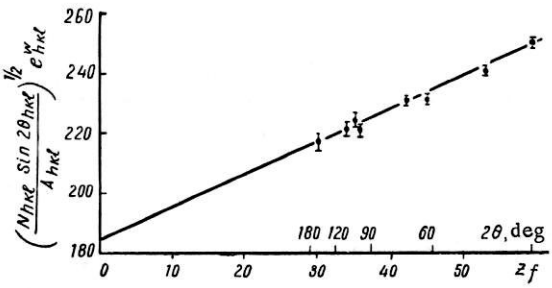

Fig. 14. $(N_{\bar{h}k\ell} \sin 2\theta_{hk\ell}/A_{hk\ell})^{1/2} e^{W hk\ell}$ as function of Zf.

effect of neutron capture in bismuth and impurities. Hence, despite the high statistical accuracy of this method, its over-all accuracy is low. The most accurate value $V_0 = -(4340 \pm 140)$ eV was obtained by this method in [84]; the cited error is the statistical error.

A more accurate experimental method of investigating ne interaction is the method of balancing the nuclear scattering amplitudes by reflection from a mirror. This method was used in [85, 86]. It is known that the refractive index of a substance for neutrons with wavelength λ is given by the relationship:

$$n^2 = 1 + \frac{\lambda^2}{\pi} \sum a_i N_i, \tag{42}$$

where N_i is the number of particles of type i per cm^3 of substance; a_i is the coherent (forward) scattering length for neutrons by particles of type i. For the ne interaction case of interest to us

$$n^2 = 1 + \frac{\lambda^2}{\pi} N (a + Z a_{ne})^*. \tag{43}$$

For accurate determination of the relative refractive index of two substances the critical angle θ_c for total reflection at their interface is measured, and

$$\theta_C^2 = n_A^2 - n_B^2 \quad (\text{for } \theta_C \ll 1), \tag{44}$$

where n_A and n_B are the refractive indices of the two substances. For liquid oxygen and bismuth we obtain from relationships (43) and (44)

$$\frac{\pi}{\lambda^2} \theta_C^2 = N_{Bi} a_{Bi} \left(\frac{N_O a_O}{N_{Bi} a_{Bi}} - 1 \right) - (N_{Bi} Z_{Bi} - N_O Z_O) a_{ne}, \tag{45}$$

where a_O and a_{Bi} are the coherent scattering amplitudes for oxygen and bismuth. Nuclear scattering on oxygen is only 2% more than on bismuth, whereas electronic scattering on bismuth, owing to its high Z, is much greater than on oxygen. Consequently, the measured critical angle θ_c is determined approximately equally by the unbalanced nuclear scattering and ne interaction. This angle is a few minutes.

The setup of the experiment carried out by Hughes et al. [85, 86] is shown in Fig. 13. The amplitudes a_O and a_{Bi} (or, more accurately, a_{Bi} and the ratio a_O/a_{Bi}) were determined from measurements of the free-atom cross sections at energies of the order of 10 eV. At these energies there is no ne interaction, since its form factor is practically zero. For conversion to coherent amplitudes a_{Bi} and a_O it was necessary to determine the spin-dependent incoherent scattering in bismuth. This was done by means of separate experiments with long-wavelength neutrons, for which there is only incoherent scattering. This led to the following value of V_0:

$$V_0 = -(3860 \pm 370) \text{ eV}. \tag{46}$$

The reflection method has an advantage over the other methods, since the measured effect is largely due to ne interaction. However, as in [82-84] the final result of the experiments [85, 86] rests on the assumption that in the energy region from 10 eV to thermal energies the amplitude is independent of the

*Since we are dealing with small-angle (forward scattering the form factor $f(\sin\theta/\lambda) = 1$.

neutron energy. Yet, as Halpern [87] reported, at energies of the order of 10 eV inelastic scattering can occur on bismuth and on oxygen. If this is so the values of a_O and a_{Bi} will differ from the values used by Hughes and the final results of the experiment would be altered accordingly. It is also essential to ensure that there is no effect due to resonances in this energy region. Nevertheless, the closeness of the results obtained by the three different experimental methods indicates that they are probably close to the true values.

Recently Koester et al. in Munich [88] made very accurate measurements of the coherent scattering amplitude for bismuth on a gravitational neutron refractometer [89] and found $a_{Bi}=(8.5234\pm0.0014)\cdot10^{-13}$ cm. This amplitude was compared with scattering cross section data at neutron energy 5.2 eV, which led to the value

$$V_0=-(4100\pm100)\,. \tag{47}$$

Table 2 gives the results of measurements of ne interaction during the period from 1947 through 1968.

Theoretical Analysis of ne Interaction. The experimentally obtained value of V_0 was explained by Foldy [90-93]. Foldy showed that in addition to the effect due to the existence of a cloud of charged virtual particles around the neutron there must be a magnetic effect, which is to be expected simply on the basis that the free neutron satisfies the Dirac equation and has an anomalous magnetic moment. A free Dirac particle does not move along a straight line, but "dances" with the velocity of light around a point which moves uniformly with velocity v. The "dance" of the particle covers a region of radius $\hbar/mc$. In the case of an electron, for instance, with charge e this movement is equivalent to a small loop with a current and in the presence of a magnetic field the electron behaves as if it had a normal magnetic moment of $e\hbar/2mc$. We can also expect effects due to the fact that the motion of the charge is not the same as that expected for a point particle, but resembles the motion of a charge distributed over a finite volume. This effect leads to a further shift of the S-electron levels in the hydrogen atom and is provided for in the Dirac theory by the term proposed by Darwin [94]. Thus, the "vibration" of a point electron leads to an apparent finite extension of its charge distribution and to a normal magnetic moment.

If the particle has an internal electromagnetic structure the apparent spatial extension of the charge is made up of the internal extension and the additional "smearing" due to the vibration. If we are to obtain information about the internal structure of the neutron from experimental ne-interaction data we have to separate the contribution made by vibration.

The scattering amplitude of a Dirac particle on a weak, slowly varying, purely electrostatic potential $\varphi(\mathbf{r})$ was obtained by Foldy [93] from the generalized Dirac equation [91, 95, 96]:

$$\gamma_\mu\frac{\partial\Psi}{\partial x_\mu}+\frac{Mc}{\hbar}\psi-\frac{i}{\hbar c}\sum_{n=0}^{\infty}\left[\varepsilon_n\gamma_\mu\Box^n A_\mu+\frac{1}{2}\mu_n\gamma_\mu\gamma_\nu\Box^n\left(\frac{\partial A_\mu}{\partial x_\nu}-\frac{\partial A_\nu}{\partial x_\mu}\right)\right]\psi=0, \tag{48}$$

where ε_0 is the total charge of the Dirac particle; μ_0 is the anomalous magnetic dipole moment of the Dirac particle in the form introduced by Pauli [97].

The remaining terms in these series are the higher radial moments of the internal charge distribution and the current due to the particle. In particular, the term with coefficient ε_1 represents the radial extension of the internal charge distribution, while the coefficient ε_1 is connected with the rms electric radius by:

$$\varepsilon_1\sim\frac{1}{6}\int r^2\rho(\mathbf{r})\,d\mathbf{r}=\frac{e}{6}\langle r_e^2\rangle. \tag{49}$$

The term with μ_1 is due to the radial extension of the magnetic moment of the particle.

Thus, in the first Born approximation the scattering amplitude will have the form [93]

$$a(\mathbf{k})=-\frac{M}{2\pi\hbar^2}\int e^{-i\,\mathbf{kr}}\sum_{n=0}^{\infty}\left[\varepsilon_n+\frac{\hbar}{2Mc}\mu_{n-1}+\frac{1}{2}\left(\frac{\hbar}{2Mc}\right)^2\varepsilon_{n-1}+\ldots\right]\Delta^n\varphi(\mathbf{r})\,d\mathbf{r}\,, \tag{50}$$

where $\hbar\mathbf{k}$ is the momentum transfer in scattering.

In the case of small momentum transfers there is only the term with n=0, which gives the electrostatic scattering on a point charge ε_0:

$$a_0(\mathbf{k}) = -\frac{M\varepsilon_0}{2\pi\hbar^2}\int e^{i\,\mathbf{kr}}\,\varphi(\mathbf{r})\,d\mathbf{r} \tag{51}$$

and n=1;

$$a_1(\mathbf{k}) = -\frac{M}{2\pi\hbar^2}\left[\varepsilon_1 + \frac{\hbar}{2Mc}\mu_0 + \frac{1}{2}\left(\frac{\hbar}{2Mc}\right)^2\varepsilon_0\right]\int e^{i\,\mathbf{kr}}\,\nabla^2\varphi(\mathbf{r})\,d\mathbf{r}. \tag{52}$$

In the case of the neutron $\varepsilon_0=0$, and $a_1(k)$ is entirely responsible for the observed ne interaction. For the required ne scattering amplitude we obtain ($k \to 0$)

$$a_{ne} = -\frac{2Me}{\hbar^2}\left(\varepsilon_1 + \frac{\hbar}{2Mc}\mu_0\right). \tag{53}$$

In this expression the term containing ε_1 is due to the radial extension of the charge distribution in the neutron. The term with μ_0 is the magnetic contribution and is due to the vibration of a particle having an anomalous magnetic moment μ_0.

As was related in [98], Weisskopf gave a simple semiqualitative interpretation of the effect. The trajectory of the moving neutron is a spiral along which it moves with the velocity of light c so that the transport velocity is equal to the velocity ν. When the neutron is at a distance $R \leq \hbar/Mc$ from the electron, magnetic spin-orbit interaction between the electron current and the magnetic moment of the neutron will occur. A calculation of this interaction shows that it agrees, aside from the factor 3/4, with Foldy's result.

By using (39) we can obtain from (53)

$$V_0 = 3e\left(\frac{mc^2}{e^2}\right)^3\left(\varepsilon_1 + \frac{\hbar}{2Mc}\mu_0\right) = V_{0\varepsilon_1} + V_{0\mu_0}. \tag{54}$$

Substitution of the numerical values gives $V_{0\mu_0} = -4080$ eV.

A comparison of this value with the experimental data of Table 2 shows that the majority of measurements, apart from those of [81, 84], which strongly contradict one another, agree within the limits of error with the value of $V_{0\mu_0}$. Thus, the determination of the contribution of $V_{0\varepsilon_1}$ or, in other words, the measurement of $\langle r_e^2\rangle_n$, will necessitate an increase in the accuracy of the measurements. It would be even better, however, to use some new, more sensitive technique. All that we can say at present about the value of $\langle r_e^2\rangle_n^{1/2}$ is that it is small and evidently does not exceed $0.1\cdot10^{-13}$ cm.* It is of interest to note that if the neutron has the same $\langle r_e^2\rangle_n$ as the proton, then, as the calculations of [99] show, for $V_{0\varepsilon_1}$ we would obtain a value of $V_{0\varepsilon_1} \sim 16{,}000$ eV.

The amplitude a_{ne} (or the equivalent potential V_0) can be expressed in terms of the neutron electric form factor G_{En}. Differentiating expression (21) with respect to q^2 and using (19) we obtain

$$\left(\frac{\partial G_{En}}{\partial q^2}\right)_{q^2=0} = \frac{\langle r_e^2\rangle_n}{6} + \varkappa\frac{\hbar^2}{4M^2c^2}. \tag{55}$$

Taking (49) into account and comparing (55) and (54) we obtain

$$\left(\frac{\partial G_{En}}{\partial q^2}\right)_{q^2=0} = \frac{V_0}{3e^2}\left(\frac{e^2}{mc^2}\right)^3. \tag{56}$$

Thus, by investigating ne interaction we can obtain the value of $\left(\frac{\partial G_{En}}{\partial q^2}\right)_{q^2=0}$. The main contribution to $\left(\frac{\partial G_{En}}{\partial q^2}\right)_{q^2=0}$ is due to the magnetic term, equal to $\varkappa\hbar/4M^2c^2 = 0.0210f^2$. The contribution of the term containing $\langle r_e^2\rangle_n$ is still obscure.

Investigation of ne Interaction from Neutron Diffraction by a Tungsten Crystal. As already mentioned, if any conclusions regarding the contribution of the term containing ε_1 to the ne scattering amplitude

*The corresponding value for the proton is $\sim 0.8\cdot10^{-13}$ cm [99].

are to be made, the accuracy of the measurements will have to be increased from 10% to 1–2%. Measurements made to an accuracy of 3% by various methods [81, 84, 88], however, lead to results which differ from one another by more than four errors and give values of ε_1 which differ even in sign.

The main defect of these methods is the very small value of the observed effect in comparison with the strong neutron-nucleus interaction. Hence, there is always the risk of some unconsidered nuclear effect affecting the results. For instance, in the case of measurements with bismuth a change of only 1/1000 in the nuclear cross section of bismuth between 0 and 10 eV leads to a 10% change in the measured ne interaction amplitude. In measurements of a half per cent effect to an accuracy of better than 3% on noble gases one must be absolutely sure that there are no other effects (e.g., p resonances, admixtures of light gases, etc.) which cause false asymmetry. In view of this it is of interest to find a new method of investigating ne interaction in which the measured effect is greater. Since the relative contribution to the scattering cross section from ne interaction is $\Delta\sigma/\sigma \sim Z\Delta f\, a_{ne}/a_N$, the measurements should be made on a heavy nucleus with small a_N.

It was reported in [100] that owing to the interference of potential and resonance scattering the isotope ^{186}W must have an anomalously small nuclear scattering amplitude in the region of neutron thermal energies. It was suggested that a_{ne} should be determined from an investigation of neutron diffraction in a mixture enriched with this isotope. Since tungsten metal is a paramagnetic [76], magnetic scattering should not make any contribution to the diffraction peaks [75, 76]. In [101] the single-crystal neutron diffraction technique was used to determine the energy dependence (in the range 0.008–0.13 eV) of the nuclear scattering amplitude of a mixture containing 90.7% ^{186}W. In the analysis of the results of these measurements the authors had to take into account ne scattering, the contribution of which to the total amplitude was about 20%.

Measurements of the intensities of the Bragg reflections of monochromatic neutrons with wavelength 1.15 Å from a single crystal containing 90.7% ^{186}W* have been made. The intensity of each reflection is

$$N_{hkl}\left(\frac{\sin\theta}{\lambda}\right) = k\left\{\left[a_я + Zf\left(\frac{\sin\theta}{\lambda}\right)_{hkl} a_{ne}\right]^2 + \left[1 - f\left(\frac{\sin\theta}{\lambda}\right)_{hkl}\right]^2 \gamma^2 \operatorname{ctg}^2\theta\right\} A_{hkl}\frac{e^{-2W_{hkl}}}{\sin 2\theta_{hkl}}, \qquad (57)$$

where k is a constant for all the measured reflections; a_N is the nuclear scattering amplitude; A_{hkl} is the absorption factor determined by calculation; e^{-2W} is the Debye-Waller factor, which takes into account the thermal vibrations of the atoms in the lattice; $W=B(\sin\theta/\lambda)^2$, where B=const for all the measured reflections; θ_{hkl} is the glancing angle; and lastly, the term containing $\gamma^2\cot^2\theta$, where $\gamma = 1/2x_n(-\hbar/Mc)(Ze^2/\hbar c)$, represents the Schwinger scattering.

The intensities of eight reflections [(110), (200), (220), (310), (400), (330), (420), and (510)] were determined experimentally. The values of the Debye-Waller factor were determined from a calculation based on [102, 103]. The analysis of the phonon spectrum of tungsten made in these investigations led to a value $B=0.147$ Å^2, which corresponds to the Debye temperature $\theta_D=355°K$. Since the contribution of Schwinger scattering to (57) does not exceed 3% it can be neglected in a first approximation. Then the quantity

$$\left(\frac{N_{hkl}\sin 2\theta_{hkl}}{A_{hkl}}\right)^{1/2} e^{W_{hkl}} = k^{1/2}(a_я + Zf_{hkl}\, a_{ne})$$

will depend linearly on Zf. In Fig. 14 this relationship is illustrated by one of the series of measurements. Figure 14 shows that a_N and a_{ne} have the same sign. This agrees with the results of measurements of [10], which showed that a_N is negative for this isotopic mixture. The observed scattering asymmetry is due to ne interaction and is

$$R-1 = \frac{(a_N + f_{(110)}Za_{ne})^2}{(a_N + f_{(510)}Za_{ne})^2} \approx .019.$$

i.e., almost 40 times greater than the corresponding effect in the case of Xe.

*This work was carried out by Yu. A. Aleksandrov, A. M. Balagurov, T. A. Machekhina, G. S. Samosvat, L. N. Sedlakova (JINR), and N V. Rannev and L. E. Fykin (Physicochemical Institute).

A least-squares treatment of equations of the type (57) for the eight measured reflections gave the value of the ratio a_{ne}/a_N. Specially conducted experiments with W powders (with natural and investigated isotope mixtures) gave the total scattering amplitude for the (110) reflection. These experiments were carried out on two different apparatuses with two sets of specimens prepared by different methods and gave similar results. The value of a_{ne} is determined by comparing the total amplitude for the (110) reflection with the ratio a_{ne}/a_N.

The obtained value of a_{ne} differed excessively from the results of previous measurements. Hence, attempts were made to find the reason for this large discrepancy. In particular, the authors carried out experiments in which the dimensions of the neutron beam reflected from the crystal were measured and their variation from reflection to reflection was determined. The dimensions of the beam were much less than the angular opening of the detector and the variation with Bragg angle was insignificant. Since the crystal of enriched tungsten was grown from a natural seed the natural tungsten might have diffused into the enriched tungsten and led to variation of a over the height of the crystal. This hypothesis was tested by measuring the intensities of the reflections from the upper and lower halves of the investigated specimen (the specimen was oriented along the direction of growth of the crystal). No differences between the slopes of the straight lines (see Fig. 14), which determine the ratio a_{ne}/a_N, were found. Nevertheless, it is intended to carry out a further analysis of the isotopic composition of the crystal used. The results of the measurements might also have been affected by effects associated with magnetic scattering of neutrons, effects which were absent in previous experiments. These effects are now being assessed.

It is possible that B was incorrectly determined: this would have a significant effect on the final result. In particular, the value $a_{ne} = -1.45 \cdot 10^{-16}$ cm (V_0=4080 eV) could be obtained from the measurements if B is taken as 0.26 Å^2 ($\theta_D \approx 270$°K). In view of this, direct experimental determination of B for W is extremely desirable.

The effect of magnetic scattering was investigated in experiments aimed at detecting ordered magnetic moments in W atoms. Such experiments were undertaken earlier and consisted in a search for the (100) reflection from powdered samples of natural W [104]. These measurements indicated that $\mu_W < 0.3$ μ_B, where μ_B is the Bohr magneton. Similar measurements made on a single crystal of a mixture enriched with ^{186}W (90.7%) at room temperature gave $\mu_W \lesssim 0.004$ μ_B.

LITERATURE CITED

1. R. Marshak and E. Sudarshan, Introduction to Elementary Particle Physics, Interscience Publ., New York (1961).
2. G. Feinberg and M. Goldhaber, Proc. Nat. Acad. Sci., U.S.A., 45, 1301 (1959).
3. P. Dee, Proc. Roy. Soc., (London), A136, 727 (1932).
4. I. S. Shapiro and I. V. Éstulin, Zh. Éksp. Teor. Fiz., 30, 579 (1956).
5. J. King, Phys. Rev. Lett., 5, 562 (1960).
6. V. Hughes, Phys. Rev., 105, 170 (1957).
7. J. C. Zorn etel., Phys. Rev., 129, 2566 (1963).
8. C. G. Shull et al., Phys. Rev., 153, 1415 (1967).
9. R. A. Lyttleton and H. Bondi, Proc. Roy. Soc. (London), A252, 313 (1959); A257, 442 (1960).
10. A. Piccard and E. Kessler, Arch. Sci. Phys. Nat., 7, 340 (1925); P. Blackett, Nature, 159, 658 (1947); V. A. J. Bailey, Proc. Roy. Soc. (London), 97, 77 (1960).
11. M. A. Markov, Zh. Éksp. Teor. Fiz., 51, 878 (1966); High-Energy Physics and Elementary Particle Theory [in Russian], Naukova Dumka, Kiev (1967), p. 671; in: Proceedings of International Seminar on Elementary Particle Theory, Varna, May 6-9, 1968; Preprint JINR R2-4050, Dubna (1968); Preprint JINR R2-4534, Dubna (1969).
12. L. D. Landau and E. M. Lifshits, Field Theory [in Russian], Nauka, Moscow (1967), p. 434.
13. Yu. B. Rumer, Investigations on 5-Optics [in Russian], Gostekhteorizdat, Moscow (1956).
14. L. D. Landau, Zh. Éksp. Teor. Fiz., 32, 405 (1957).
15. J. Smith et al., Phys. Rev., 108, 120 (1957).
16. P. D. Miller et al., Phys. Rev. Lett., 19, 381 (1967).
17. P. Miller, Usp. Fiz. Nauk, 95, 470 (1968).
18. P. D. Miller et al., 14th Internat. Conf. on High-Energy Physics, Vienna (1968), p. 300.
19. C. G. Shull and P. Nathans, Phys. Rev. Lett., 19, 384 (1967).
20. Yu. A. Aleksandrov et al., Preprint JINR R3-4121, Dubna (1968).

21. F. L. Shapiro, Usp. Fiz. Nauk, 95, 145 (1968).
22. S. D. Drell and F. Zachariasen, Electromagnetic Structure of Nucleons, O.U.P., London (1961).
23. V. K. Fedyanin, Electromagnetic Structure of Nuclei and Nucleons [in Russian], Vysshaya Shkola, Moscow (1967).
24. E. J. Ernst et al., Phys. Rev., 119, 1105; R. G. Sachs, Phys. Rev., 126, 2256 (1962); L. N. Hand et al., Phys. Rev. Lett., 8, 110 (1962).
25. Proc. Internat. Symp. on Electron and Proton Interactions at High Energies, Stanford, California, September 5-9, 1967, p. 70-71.
26. G. Berger et al., 14th Internat. Conf. on High-Energy Physics, Vienna, 1968, p. 516.
27. G. Höhler et al., 14th Internat. Conf. on High-Energy Physics, Vienna, 1968, p. 233.
28. A. Klein, Phys. Rev., 99, 998 (1955).
29. A. M. Baldin, Nucl. Phys., 18, 310 (1960).
30. Yu. A. Aleksandrov and I. I. Bondarenko, Zh. Éksp. Teor. Fiz., 31, 726 (1956).
31. V. S. Barashenkov et al., Zh. Éksp. Teor. Fiz., 32, 154 (1957).
32. V. I. Gol'danskii et al., Zh. Éksp. Teor. Fiz., 38, 1965 (1960).
33. I. L. Powell, Phys. Rev., 75, 32 (1949).
34. M. Gell-Mann and M. Goldberger, Phys. Rev., 96, 1433 (1954).
35. V. A. Petrun'kin, Zh. Éksp. Teor. Fiz., 40, 1148 (1960).
36. V. S. Barashenkov et al., Preprint JINR R-1348, Dubna (1963).
37. V. A. Petrunkin, Nucl. Phys., 55, 197 (1964).
38. L. I. Lapidus, Preprint JINR R-967, Dubna (1962).
39. Yu. A. Aleksandrov and G. S. Samosvat, Preprint JINR R-2495, Dubna (1965).
40. V. S. Barashenkov et al., Nucl. Phys., 50, 684 (1964).
41. G. F. Chew, Phys. Rev., 80, 196 (1950); G. F. Chew and M. Goldberger, Phys. Rev., 87, 778 (1952); R. Capps, Phys. Rev., 106, 1031 (1957).
42. A. Tenore and A. Verganelakis, Nuovo Cimento, 35, 261 (1965).
43. L. I. Lapidus and Chou Kuang-chao, Zh. Éksp. Teor. Fiz., 39, 1286 (1960).
44. R. S. Jones et al., Phys. Rev., 128, 1357 (1962); J. Fox et al., Bull. Amer. Phys. Soc., 9, 69 (1964).
45. G. Bernardini, 9th Internat. Annual Conf. on High-Energy Physics, Kiev, 1959.
46. L. G. Moroz and V. N. Tret'yakov, Dokl. Akad. Nauk BSSR, 8, 575 (1964).
47. Yu. A. Aleksandrov, Zh. Éksp. Teor. Fiz., 33, 294 (1957).
48. Yu. A. Aleksandrov et al., Zh. Éksp. Teor. Fiz., 40, 1878 (1961).
49. Yu. V. Dukarevich and A. N. Dyumin, Zh. Éksp. Teor. Fiz., 44, 130 (1963).
50. V. S. Barashenkov and B. M. Barbashov, Nucl. Phys., 9, 426 (1958).
51. V. S. Barashenkov and G. Yu. Kaizer, Preprint JINR R-771, Dubna (1961).
52. G. Breit and M. Rustgi, Phys. Rev., 114, 830 (1959).
53. T. Vela and M. Samawara, Progr. Theoret. Phys., 24, 519 (1960).
54. A. Kazanawa, Nucl. Phys., 24, 524 (1961).
55. M. Walt and D. Fossan, Phys. Rev., 137, B629 (1965).
56. G. V. Anikin et al., Nuclear Structure Study with Neutrons, Antwerp, 19-23 July, 1965, p. 574.
57. J. Monahan et al., Nuclear Structure Study with Neutrons, Antwerp, 19-23 July, 1965, p. 588; A. J. Elwyn et al., Phys. Rev., 142, 758 (1966).
58. G. V. Gorlov et al., Yadernaya Fizika, 8, 1086 (1968).
59. A. Adam et al., Nuclear Structure Symposium, Dubna, July 4-11, 1968.
60. F. T. Kuchnir, et al., Phys. Rev., 176, 1405 (1968).
61. Yu. A. Aleksandrov, Dissertation, FÉI (1959).
62. V. M. Koprov and L. N. Usachev, "Nuclear reactions at low and medium energies," in: Proceedings of All-Union Conference, 1960 [in Russian], Izd-vo AN SSSR, Moscow.
63. V. M. Agranovich and D. D. Odintsov, Proceedings of All-Union Conference, 1960 [in Russian] Izd-vo AN SSSR, Moscow.
64. A. N. Dyumin, Dissertation, Physicotechnical Institute (1964).
65. R. M. Thaler, Phys. Rev., 114, 827 (1959).
66. Yu. A. Aleksandrov et al., ZhÉTF Pis. Red., 4, 196 (1966).
67. M. Goldberg et al., BNL-400, Second edition, Vol. 11 (1962).
68. S. B. Gerasimov et al., Zh. Éksp. Teor. Fiz., 43, 1872 (1962).

69. V. S. Barashenkov and H. J. Kaiser, Nucleon Structure, Proc. of Internat. Conf. at Stanford Univ., June 24-27, 1963, p. 263.
70. V. S. Barashenkov, Internat. Winter School of Theoretical Physics in JINR, Vol. 3 [in Russian], JINR, Dubna (1964), p. 86.
71. G. de Vries et al., Preprint Stanford Univ. (1963).
72. W. K. H. Panofsky, 14th Internat. Conf. on High-Energy Physics, Vienna, August 28-September 5, 1968, p. 23.
73. V. S. Barashenkov et al., Preprint JINR R-2894, Dubna (1966).
74. R. P. Zaikov, Preprint JINR R2-3073, Dubna (1966).
75. D. Hughes, Neutron Optics, Interscience Publ., New York (1955).
76. G. Bacon, Neutron Diffraction, Clarendon Press, Oxford (1962).
77. A. H. Compton and S. K. Allison, X Rays in Theory and Experiment, New York (1957).
78. E. Fermi and L. Marshall, Phys. Rev., 72, 1139 (1947).
79. M. Hamermesh et al., Phys. Rev., 85, 483 (1952).
80. M. F. Crouch et al., Phys. Rev., 102, 1321 (1956).
81. V. Krohn and G. Ringo, Phys. Rev., 148, 1303 (1966).
82. W. Havens et al., Phys. Rev., 72, 634 (1947).
83. W. Havens et al., Phys. Rev., 82, 345 (1951).
84. E. Melkonian et al., Phys. Rev., 114, 1571 (1959).
85. J. Harvey et al., Phys. Rev., 87, 220 (1952).
86. D. Hughes et al., Phys. Rev., 90, 497 (1953).
87. O. Halpern, Phys. Rev., 133, B581 (1963).
88. L. Koester, Technische Hochschule, Munich (private communication) (1969).
89. L. Koester, Z. Phys., 182, 328 (1965); L. Koester, Z. Phys., 198, 187 (1967).
90. L. Foldy, Phys. Rev., 83, 688 (1951).
91. L. Foldy, Phys. Rev., 87, 688 (1952).
92. L. Foldy, Phys. Rev., 87, 693 (1952).
93. L. Foldy, Rev. Mod. Phys., 30, 471 (1958).
94. C. G. Darwin, Proc. Roy. Soc. (London), A118, 654 (1928).
95. G. Salzman, Phys. Rev., 99, 973 (1955).
96. A. C. Zemach, Phys. Rev., 104, 1771 (1957).
97. W. Pauli, Relativistic Theory of Elementary Particles [Russian translation], Izd-vo Inostr. Lit., Moscow (1947).
98. E. Segrè (Ed.), Experimental Nuclear Physics, John Wiley & Sons, New York (1953).
99. D. R. Yenny et al., Rev. Mod. Phys., 29, 144 (1957).
100. Yu. A. Aleksandrov, Preprint JINR R3-3442, Dubna (1967).
101. Yu. A. Aleksandrov et al., Preprint JINR R3-4121, Dubna (1968).
102. P. S. Mahesh and B. Dayal, Phys. Rev., 143, 443 (1966).
103. F. H. Chem and B. N. Brockhouse, Solid State Commun., 2, 73 (1964).
104. C. G. Shull and M. K. Wilkinson, Rev. Mod. Phys., 25, 100 (1953).